Novel methodology utilizing confocal laser scanning microscopy for systematic analysis in arthropods (Insecta)

Angela V. Klaus[1,*] and Valerie Schawaroch[†,§]

[*]Microscopy and Imaging Facility and †Division of Invertebrate Zoology, American Museum of Natural History, Central Park West at 79th Street, New York, NY 10024-5192, USA; [§]Department of Natural Sciences, Baruch College, 1 Bernard Baruch Way, Box A-0506, New York, NY 10010-5585, USA

Synopsis The use of confocal laser scanning microscopy (CLSM) for imaging arthropod structures has the potential to profoundly impact the systematics of this group. Three-dimensional visualization of CLSM data provides high-fidelity, detailed images of minuscule structures unobtainable by traditional methods (for example, hand illustration, bright-field light microscopy, scanning electron microscopy). A CLSM data set consists of a stack of 2-D images ("optical slices") collected from a transparent, fluorescent specimen of suitable thickness. Small arthropod structures are particularly well suited for CLSM imaging owing to the autofluorescent nature of their tissues. Here, we document the practical aspects of a methodology developed for obtaining image stacks via CLSM from autofluorescent insect cuticular structures.

Introduction

The first confocal laser scanning microscopes became commercially available in 1987 (for a review, see Amos and White 2003), 30 years after the invention of the instrument by Marvin Minsky in 1957 (Minsky 1961). Minsky's original instrument relied on stage scanning and a white-light illumination source, whereas modern instruments exploit beam scanning of a monochromatic laser light source. The key concept behind confocal laser scanning microscopy is the microscope's ability to obtain clear optical sections (as opposed to physical tissue sections) of transparent, fluorescent specimens. This capability allows for the collection of a stack of 2-D images obtained from sequential focal planes within a 3-D object (for an overview, see Murphy 2001). The "optical sectioning" capability of CLSM is a result of the incorporation of a physical aperture, or pinhole, into the path of light being emitted from the specimen. The confocal pinhole is placed in front of the detector (a photomultiplier tube) in an image plane that is conjugate with the specimen plane so that only in-focus light from the specimen is collected; out-of-focus light is largely blocked from detection. Thus, when a CLSM data set is reconstructed into a 3-D object, blur from out-of-focus light is eliminated, and a clear rendering of the original object is obtained.

CLSM mainly relies on signals from fluorescent molecules. Confocal imaging using a reflected light signal is also possible, but the technique is not as commonly used for biological purposes and is beyond the scope of this article (for a review, see Paddock 2002). Fluorescence CLSM is integral to research in cell biology, developmental biology, and neuroscience, where the technique is used to visualize molecules or structures within cells or tissues. In typical biological CLSM applications, structures are labeled with fluorescent dyes using a number of well-developed techniques, including immunofluorescence labeling, microinjection, and expression of proteins of interest bound to natural fluorescent reporter molecules such as green fluorescent protein (for an overview of these techniques, see Paddock 1999).

Rather than relying on labeling with exogenous dyes, the approach described in the current study takes advantage of the natural endogenous fluorescence (autofluorescence) exhibited by the arthropod cuticle. The exact chemical source of this fluorescence is unknown; however, a number of components isolated from insect cuticles including pteridines (Lardeux and others 2000) and the protein resilin (Neff and others 2000) have autofluorescent properties. Few studies have exploited the autofluorescent property of the cuticle material for systematics analysis. Morphologists require detailed and highly resolved representations of diagnostic structures to assist in identifying potential characteristics, to facilitate hypotheses of homology, and to accurately communicate these structures to

From the symposium "The New Microscopy: Toward a Phylogenetic Synthesis" presented at the annual meeting of the Society for Integrative and Comparative Biology, January 4–8, 2005, at San Diego, California.

[1] E-mail: avklaus@amnh.org

Integrative and Comparative Biology, volume 46, number 2, pp. 207–214
doi:10.1093/icb/icj015
Advance Access publication February 16, 2006

other scientists. Galassi (1997a, 1997b) and Galassi and colleagues (1998) documented structural characters of copepod integumental structures using CLSM for taxonomic diagnosis. These were the first papers to use confocal imaging in arthropod systematics; however, other examples have been lacking in the literature. We have found CLSM to be useful in documenting minuscule insect structures (Klaus and others 2003; Schawaroch and others 2005). The approach we describe in the current work is novel in that it provides a strategy for data collection that allows for advanced 3-D visualization of structures. We describe the mounting and imaging procedures necessary to minimize aberration artifacts inherent in confocal imaging of thick specimens and show that optical sectioning by CLSM of cuticular structures from several different insect species produces 3-D renderings of great clarity and accuracy.

Methods

Specimens

The *Drosophila melanogaster* specimen used was from a culture obtained from Carolina Biological Supply Company. All other insect specimens used were field-collected at the following localities: a mosquito, *Culex tarsalis*, from California, USA; drosophilid flies, *Cladochaeta inversa*, from Houghton County, Michigan, USA; *Drosophila melanica* from Black Rock Forest, Cornwall, New York, USA; a cockroach, *Lauraesilpha heteroclita*, from New Caledonia; and a new plant bug species (Family: Miridae) from Utah, USA. Specimens were preserved by air-drying, immersion in 70% ethanol, or critical-point-drying following ethanol fixation. We observed no differences in autofluorescence based on the method of tissue preservation.

Specimen mounting

As with standard bright-field light microscopy, CLSM requires that specimens be imaged through a coverslip. However, because confocal imaging is a 3-D technique, specimens are mounted in such a way as to avoid deformation (compression or crushing) of the structures of interest, usually through the use of spacers. The structures imaged in this study were prepared by mounting between 2 coverslips in either glycerin jelly (nonpermanent) or euparal (permanent)

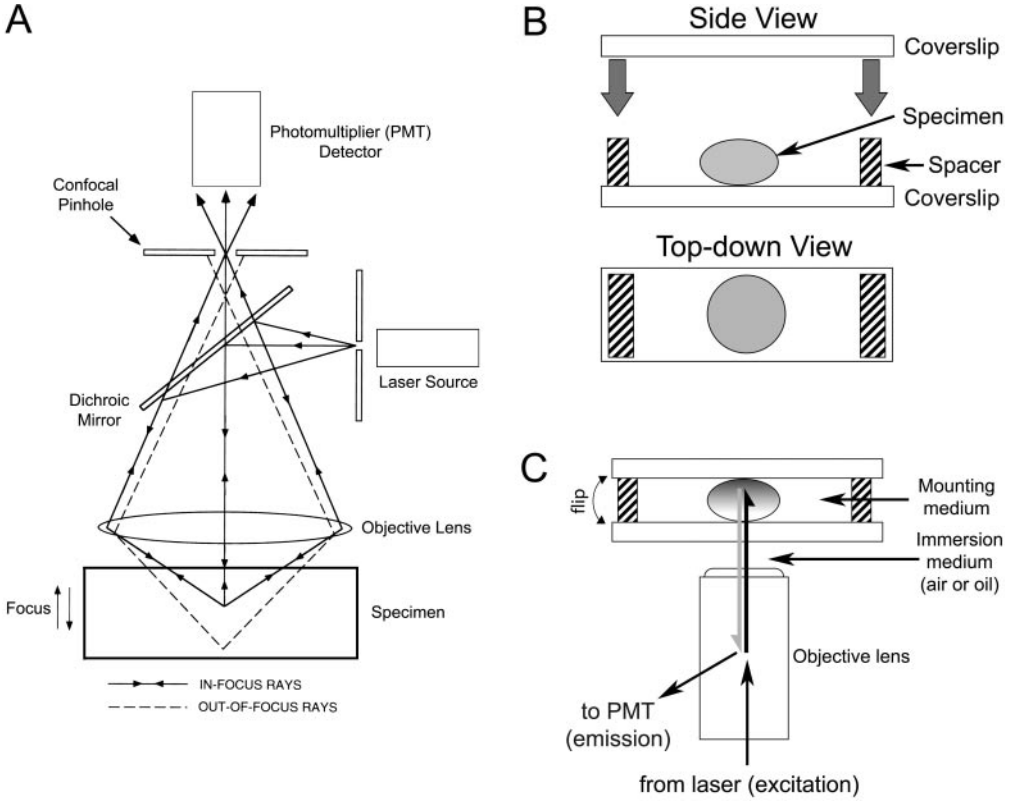

Fig. 1 (A) The confocal principle (modified from Paddock 1999, with permission). (B) Sample mounting method. (C) Confocal imaging setup. The gradient within the specimen indicates data loss from the side of the specimen farther away from the sources of illumination and detection. Confocal microscopes use epi-illumination; that is, the illumination source and the source of detection are on the same side of the specimen, and the objective lens acts as both objective and condenser.

medium. Mosquito (*Cx. tarsalis*) gonocoxites were mounted directly between the coverslips because of their flattened nature; structures from other flies (*D. melanogaster*, *D. melanica*, *C. inversa*), from the Miridae species (plant bug), and from *L. heteroclita* were mounted using coverslip spacers of known thickness in order to avoid compression. The mounting procedure is shown in Figure 1B.

Specimens were mounted between 2 coverslips, rather than on a glass slide using 1 coverslip, so that structures could be imaged from both sides by flipping the mount (Fig. 1C). This step is necessary in order to compensate for data loss from the side of the specimen farther away from the sources of illumination and detection (see Fig. 3, discussed later). Because increasing specimen thickness exacerbates aberrations in the optical setup (de Grauw and others 2002; Diaspro and others 2002), care should be taken to use just the amount of medium necessary to cover the specimens. The experimental details of specimen preparation and confocal imaging of arthropod structures are described in depth elsewhere, as are the theoretical underpinnings of the technique (Klaus and others 2003; Schawaroch and others 2005).

Confocal imaging and 3-D reconstruction

All specimens in this study were imaged on a Zeiss 510 confocal microscope equipped with a Zeiss Axiovert 100M inverted microscope. Three-dimensional visualization of structures was carried out using the 3-D projection module in the freeware version of the Zeiss LSM Image Browser software (for maximum-intensity projections, MIPs). The "keep maximum" tool was used, which combines MIP with limited alpha-blending functions. The Surpass module in the commercial software package Imaris (Bitplane Inc., Saint Paul, MN) was used for pure alpha-blended volume rendering and for surface reconstruction.

Results and discussion

The principle of confocal imaging is shown in Figure 1A. As mentioned earlier, the optical sectioning capability of CLSM is derived from the placement of the confocal pinhole in front of the photomultiplier tube. Optical slices are collected from successive focal planes by moving the specimen (or the objective lens) in the *z*, or axial, dimension. Figure 1C depicts the imaging strategy used for thick arthropod structures ("thick" in confocal imaging generally refers to specimens spanning >10 μm in the axial dimension). A confocal data set was collected from the first side of the specimen, the sample mount was flipped, and another data set was collected from the opposite side. This strategy was used in order to address the

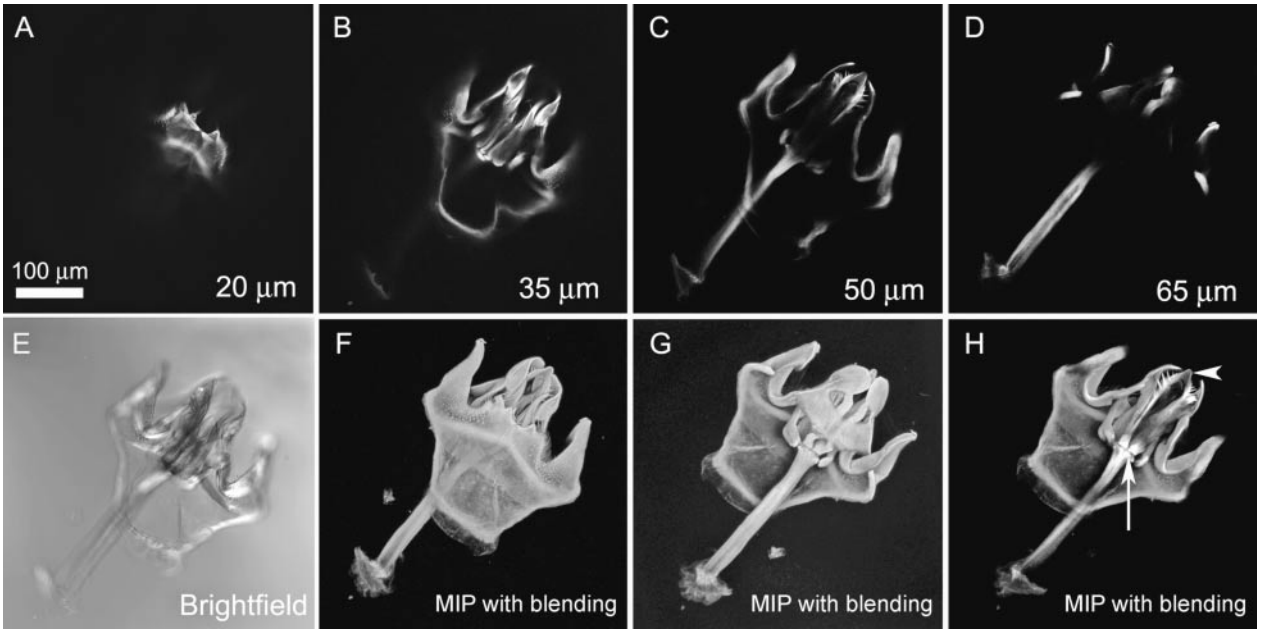

Fig. 2 *Drosophila melanogaster* phallic structures. (A–D) Confocal images from selected apparent focal depths. (E) Transmitted light bright-field image. (F and G) Maximum-intensity projections (MIPs) created from separate data sets collected from each side of the specimen mount. (H) MIP of partial image stack showing internal structures (arrowhead, aedeagus; arrow, aedeagal apodeme juncture). All MIPs (with blending) were created using the 3-D projection module in the freeware version of the Zeiss LSM Image Browser software. Scale bar = 100 μm for all panels.

problem of data loss artifacts in data sets collected from thick specimens.

Figure 2A–D shows selected optical sections extracted from a CLSM data set obtained from the phallic structures (including the aedeagus, hypandrium, and paraphyses) of *D. melanogaster*. The apparent imaging depth is noted on each image. The confocal optical section images are composed of the signal detected only from the plane of focus for each imaging depth. For comparison purposes, a bright-field image is shown in Figure 2E. This image is nonconfocal; therefore, light from nonfocal planes contributes to out-of-focus blur in the image. Figure 2F and G shows MIPs created from 2 separate CLSM data sets collected from opposite sides of the specimen mount (rendered using the Zeiss Image Browser software, see Methods). The image shown in Figure 2H is a reconstruction of a subset of optical slices that allows for the visualization of internal structures (that is, the aedeagus and aedeagal apodeme juncture, indicated by the arrowhead and the arrow, respectively).

Aberration artifacts in CLSM data sets

Aberration artifacts are difficult to avoid when imaging thick specimens by CLSM. The most commonly encountered aberrations are (1) data loss from the side of the specimen farther away from the sources of illumination and detection and (2) axial distortion (compression or elongation) of the 3-D data set. These artifacts are usually the result of increasing penetration depth and spherical aberration introduced into the imaging setup by refractive index (RI) mismatch, respectively (Diaspro and others 2002; Klaus and others 2003).

The reduction of artifacts present in 3-D data sets collected from thick specimens was addressed in the current work in 2 ways. First, as described earlier, in order to address data loss artifacts arising from increasing penetration depth, specimens were imaged from both sides by flipping the sample mount (Fig. 1C) and slides were made as thin as possible by using minimal amounts of mounting media. Second, in order to reduce RI mismatch, specimens were imaged

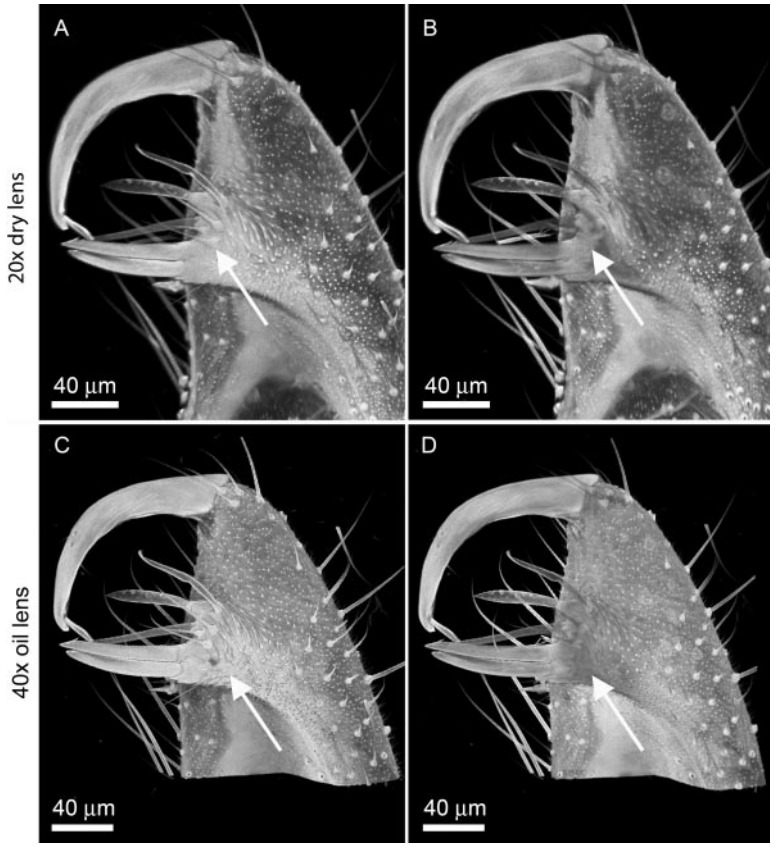

Fig. 3 Volume renderings of *Culex tarsalis* gonocoxite. (A and B) Two separate data sets collected with 20× dry objective lens. (C and D) Two separate data sets collected with 40× oil immersion lens. The arrows in panels B and D indicate regions of the specimens where data loss is most apparent (compare these with the same areas in panels A and C). All images were created using the alpha-blending function in the Surpass module of Imaris. Scale bar = 40 µm for each panel.

(whenever possible) using an oil immersion objective lens rather than a dry objective lens. These concepts are illustrated in Figures 3 and 4. Figure 3A and B shows volume renderings of 2 different data sets collected from the gonocoxite of *Cx. tarsalis* using a 20× dry objective (numerical aperture = 0.75). The same structure, shown in Figure 3C and D, was imaged using a 40× oil immersion lens (numerical aperture = 1.3). In Figure 3A and C, the side of the specimen depicted in the reconstruction was facing toward the sources of illumination and detection during imaging, whereas in Figure 3B and D, this side of the specimen was facing away. A comparison of Figure 3A and B shows significant data loss in Figure 3B (very noticeable in the region indicated by the arrow). The same situation exists between the images shown in Figure 3C and D (collected with a 40x oil immersion lens); however, the loss is not as severe. This is due to the greater RI mismatch between the mounting medium and the lens immersion medium within the optical setup when using a dry versus an oil objective lens. This specimen was mounted in euparal medium with an RI of ∼1.52. The RI of the oil used for the 40× objective was 1.51; therefore the RIs were very closely matched when using the oil immersion lens. However, when a dry lens was used, the RI of the immersion medium was 1.00 for air, causing a large RI mismatch.

Note that the data collected with the 40× oil lens have much better lateral resolution than those collected with the 20× lens as a result of the higher numerical aperture (1.3 versus 0.75 for 40× and 20× objectives, respectively).

Axial distortion is the other aberration artifact of concern when imaging thick specimens by CLSM and is mainly caused by RI mismatch. The *Cx. tarsalis* gonocoxite is used to demonstrate this concept in Figure 4. Figure 4A and B shows surface reconstructions of a gonocoxite data set obtained with a 20× dry objective lens. Figure 4A is a top-down view, and Figure 4B is a side view. The lower panel shows the same structure imaged with a 40× oil immersion lens. Note the severe compression of the entire gonocoxite when reconstructed from the 20× data set (where the RI is grossly mismatched) compared with the reconstruction from the 40× data set.

The arrow in Figure 4B indicates another form of axial distortion, that is, apparent axial elongation of small structures. This distortion is a result of extraneous signal produced above and below small structures (∼1–3 μm) when imaging with a dry objective lens (Carlsson 1991). In this example, hairs projecting from the gonocoxite have a knifelike appearance in the axial direction.

Fig. 4 Surface reconstructions of *Culex tarsalis* gonocoxite. (A and B) Top-down and side views of a data set collected with a 20× dry objective lens. Note the gross axial compression of the entire data set in panel B as a result of refractive index mismatch. The arrow in panel B indicates a hair showing apparent axial elongation owing to extraneous signal above and below the small structure (see text). (Lower panel) Stereo pair of data set collected with 40× oil immersion lens. When viewed with a stereo viewer or by slightly crossing the eyes, the 3-D nature of the reconstruction becomes apparent. The data set shown in these panels does not exhibit the severe axial compression that is seen in (B) because the refractive indices of the mounting medium and the immersion medium are closely matched. This pair was created from 2 frames taken from an animation of the structure. All surface reconstructions were created in the Surpass module of Imaris.

Data visualization

We routinely employ 3 different 3-D visualization techniques for analyzing CLSM data sets: (1) MIP with limited alpha-blending, (2) volume rendering using pure alpha-blending, and (3) isosurface reconstruction. Each technique has its own advantages for visualizing 3-D data sets. MIP is very useful because it is rapid,

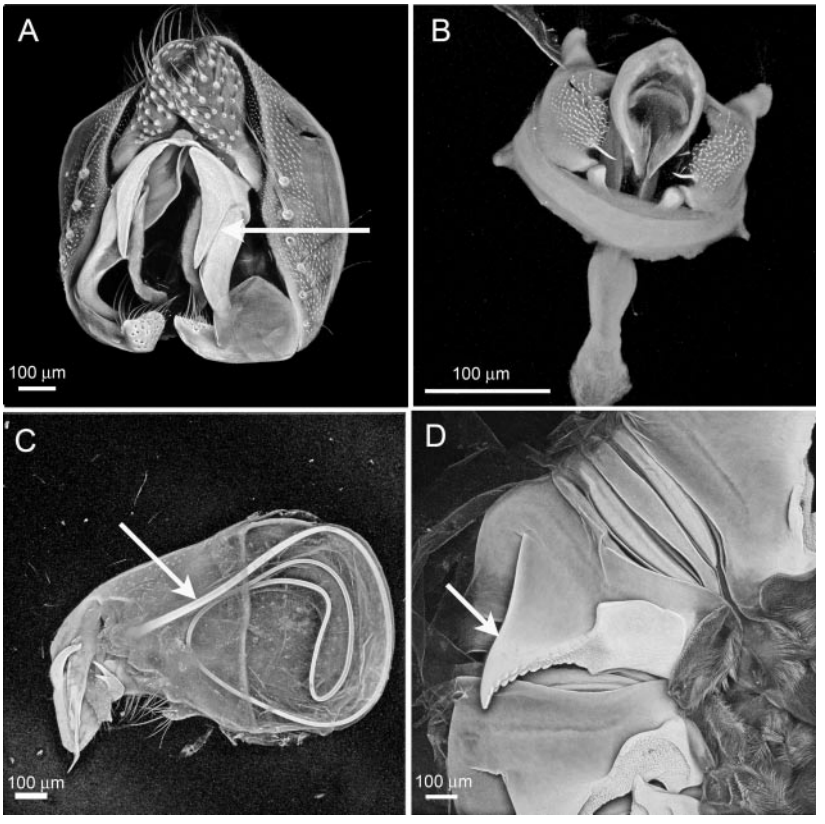

Fig. 5 Maximum-intensity projections (MIPs, with blending) of insect structures. (A) Articulated genitalic (periphallic and phallic) structures of the drosophilid fly *Cladochaeta inversa*. The arrow indicates suture between the dorsal and ventral lobes of the paraphyses. (B) Disarticulated phallic structures of the fly *Drosophila melanica*. (C) Phallic structure from a new Miridae species. The arrow indicates a duct called the vesica. (D) Gizzard structures from the cockroach, *Lauraesilpha heteroclita*. The arrow indicates a tooth. All MIPs (with blending) were created using the 3-D projection module in the freeware version of the Zeiss LSM Image Browser software.

simple, and is not computing intensive. In addition, freeware software packages (see Methods) are available with very good MIP utilities so that publication-quality data visualizations can be carried out inexpensively. MIP images, however, provide satisfactory visualizations of CLSM data sets rendered from only a limited number of viewing angles (Schreiner and others 1996; Schroeder and others 1998). More advanced volume rendering (for example, pure alpha blending) and surface reconstruction methods provide true 3-D information about a specimen. In addition, more advanced (and generally more expensive) software packages allow for viewing from all angles using interactive rotation. We have found that for the documentation of gross morphological structures, MIP with alpha-blending is adequate for most studies. Other volume rendering and surface reconstruction methods, however, allow for better visualization of internal and/or surface structures (Klaus and others 2003). Figures 2 and 5 show examples of MIP (with blending) images created using the freeware version of the Zeiss LSM Image Browser. Other volume rendered images (pure alpha-blending) and surface reconstructions created using Imaris are shown in Figures 3 and 4, respectively.

Other species visualized with CLSM

The MIPs of the structures shown in Figure 5 are highly detailed renderings and provide visualizations of exquisite external microsculpture. Figure 5A–C depicts male genitalic structures, which are important for species diagnoses and phylogenetic analyses because of their complexity and role in speciation (Eberhard 1985). Of special interest is the suture clearly visible in the *C. inversa* genitalia (arrow, Fig. 5A). This structure is not discernible using bright-field light microscopy; therefore the dorsal and ventral lobes of the paraphyses were originally interpreted as a single structure (Grimaldi and Nguyen 1999). Figure 5B and C shows portions of the male genitalic structures from another drosophilid fly (*D. melanica*) and a new Miridae species, respectively.

One of the 6 cockroach gizzard "teeth" is depicted in Figure 5D. This structure was imaged as part of a larger

morphological analysis of this species. The utility of confocal imaging over scanning electron microscopy was being tested because of the nondestructive nature of the CLSM mounting procedure in nonpermanent medium (glycerin jelly).

Conclusions

The confocal microscope provides advantages over other documentation methods (for example, hand illustration, bright-field micrography, and scanning electron microscopy) traditionally used for arthropod systematics (Schawaroch and others 2005). Documenting structures using the CLSM is a learnable technique and, as such, can supplement the talent and interpretation of features required for hand-illustrative methods. Three-dimensional reconstructions of CLSM data provide images that are free of out-of-focus blur; such images have greater depth-of-field than bright-field light micrographs, similar to images produced on a scanning electron microscope. Sample preparation for CLSM is nondestructive if specimens are mounted in nonpermanent medium. CLSM data sets have unparalleled advantages for imaging obstructions from overlying structures, and they can be rendered in a fashion so that internal structures can be revealed in situ. Additionally, once a 3-D data set is collected, it can be rotated and viewed from all angles. These advantages of CLSM over other imaging and documentation methods provide an opportunity for much improved morphological analysis of arthropod structures.

We believe this technique will be an invaluable addition to arthropod systematic investigations by way of taxonomic diagnoses, character identification, and refinement of homology statements. In this article, we have demonstrated the applicability of this CLSM imaging technique to various insects; however, it is also applicable to small arthropods, as demonstrated for copepods (Galassi 1997a, 1997b; Galassi and others 1998), ostracodes (unpublished data, V.S.), and scorpion structures (personal communication, E. Volschenk). We are hopeful that, in the future, CLSM will be incorporated into studies of all minuscule arthropods and substructures of larger organisms.

Acknowledgments

The authors gratefully acknowledge 3 anonymous referees for very helpful comments and suggestions. We also thank Varuni Kulasekera [Invertebrate Zoology, American Museum of Natural History (AMNH)] for the *Cx. tarsalis* specimen, Christiane Weirauch and Denise Wyniger (Invertebrate Zoology, AMNH) for the Miridae specimen image, Jerome Murienne (Museum National d'Histoire Naturelle, Paris) for the *L. heteroclita* image, David Grimaldi (Invertebrate Zoology, AMNH) for the *C. inversa* specimen, and Craig Gibbs (Invertebrate Zoology, AMNH) for collecting the *D. melanica* specimen. We also thank Erich Volschenk (invertebrate Zoology, AMNH) for access to unpublished data. We sincerely appreciate the outstanding software assistance and support of Jacob Mey (Microscopy and Imaging, AMNH) and Kevin Frischmann (Bitplane AG, Switzerland) in building and optimizing the data visualization computers. V.S. would like to gratefully acknowledge research support provided by National Science Foundation DEB grant #0075360 and PSC-CUNY grant #60052-34-35, as well as the Weissman School of Arts and Sciences of Baruch College, which provided release time for this work.

References

Amos WB, White JG. 2003. How the confocal laser scanning microscope entered biological research. Biol Cell 95:335–42.

Carlsson K. 1991. The influence of specimen refractive index, detector signal integration, and non-uniform scan speed on the imaging properties in confocal microscopy. J Microsc 163:167–78.

de Grauw CJ, Frederix PLTM, Gerritsen HC. 2002. Aberrations and penetration in in-depth confocal and two-photon microscopy. In: Diaspro A, editor. Confocal and two-photon microscopy: foundations, applications, and advances. New York: Wiley-Liss. p 153–69.

Diaspro A, Federici F, Robello M. 2002. Influence of refractive-index mismatch in high-resolution three-dimensional confocal microscopy. Appl Optics 41:685–90.

Eberhard WG. 1985. Sexual selection and animal genitalia. Cambridge, MA: Harvard University Press.

Galassi DMP. 1997a. The genus *Pseudectinosoma* Kunz, 1935: an update, and description of *Pseudectinosoma kunzi* sp. n. from Italy (Crustacea: Copepoda: Ectinosomatidae). Archiv für Hydrobiologie 139:277–87.

Galassi DMP. 1997b. Little known harpacticoid copepods from Italy, and description of *Parastenocaris crenobia* n. sp. (Copepoda: Harpacticoida). Crustaceana 70:694–709.

Galassi DMP, De Laurentis P, Giammatteo M. 1998. Integumental morphology in copepods: assessment by confocal laser scanning microscopy (CLSM). Fragmenta entomologica (Roma) 30:79–92.

Grimaldi D, Nguyen T. 1999. Monograph on the spittlebug flies, genus *Cladochaeta* (Diptera: Drosophilidae: Cladochaetini). Bull Am Mus Nat Hist 241:1–326.

Klaus AV, Kulasekera VL, Schawaroch V. 2003. Three-dimensional visualization of insect morphology using confocal laser scanning microscopy. J Microsc 212:107–21.

Lardeux F, Ung A, Chebret M. 2000. Spectrofluorometers are not adequate for aging *Aedes* and *Culex* (Diptera: Culicidae) using pteridine fluorescence. J Med Entomol 37:769–73.

Minsky M. 1961. U.S. patent 3013467: microscopy apparatus. Filed November 7, 1957.

Murphy D. 2001. Fundamentals of light microscopy and electronic imaging. New York: Wiley-Liss.

Neff D, Frazier SF, Quimby L, Wang RT, Zill S. 2000. Identifcation of resilin in the leg of cockroach, *Periplaneta americana*: confirmation by a simple method using pH dependence of UV fluorescence. Arthropod Struct Devel 29:75–83.

Paddock S. 1999. An introduction to confocal imaging. In: Paddock SW, editor. Confocal microscopy: methods and protocols. Totowa, NJ: Humana Press. p 1–34.

Paddock S. 2002. Confocal reflection microscopy: the "other" confocal mode. Biotechniques 32:274–7.

Schawaroch V, Grimaldi D, Klaus AV. 2005. Focusing on morphology: applications and implications of confocal laser scanning microscopy (Diptera: Campichoetidae, Camillidae and Drosophilidae). Proc Entomol Soc Wash 107:323–35.

Schreiner S, Paschal CB, Galloway RL. 1996. Comparison of projection algorithms used for the construction of maximum intensity projection images. J Comput Assist Tomogr 20:56–67.

Schroeder W, Martin K, Lorensen B. 1998. The visualization toolkit. Upper Saddle River, NJ: Prentice Hall.